The Journal of Chemical Physics

An analysis of the methyl rotation and aldehyde wagging dynamics in the S_0 ($\tilde{X}\,^1A'$) and T_1 ($\tilde{a}\,^3A''$) states of thioacetaldehyde from pyrolysis jet spectra

Cite as: J. Chem. Phys. **97**, 3964 (1992); https://doi.org/10.1063/1.462935
Submitted: 02 January 1992 . Accepted: 02 June 1992 . Published Online: 31 August 1998

D. C. Moule, H. A. Bascal, Y. G. Smeyers, D. J. Clouthier, J. Karolczak, and A. Niño

View Online Export Citation

Lock-in Amplifiers up to 600 MHz
Watch

AIP Publishing

© 1992 American Institute of Physics.

An analysis of the methyl rotation and aldehyde wagging dynamics in the S_0 ($\tilde{X}\,^1A'$) and T_1 ($\tilde{a}^3A''$) states of thioacetaldehyde from pyrolysis jet spectra

D. C. Moule[a] and H. A. Bascal
Department of Chemistry, Brock University, St Catharines, Ontario, L2S3A1, Canada

Y. G. Smeyers
Instituto de Estructura de la Materia, CSIC, c/Serrano, 119, 28006 Madrid, Spain

D. J. Clouthier and J. Karolczak[b]
Department of Chemistry, The University of Kentucky, Lexington, Kentucky 40506-0055

A. Niño
Escuela Universitaria de Informatica, Universidad de Castilla—La Mancha, Ciudad Real, 13071, Spain

(Received 2 January 1992; accepted 2 June 1992)

Jet-cooled, laser induced phosphorescence (LIP) excitation spectra of thioacetaldehyde (CH_3CHS, CH_3CDS, CD_3CHS, and CD_3CDS) have been observed in the 15 800–17 300 cm^{-1} region in a continuous pyrolysis jet. The responsible electronic transition, $T_1 \leftarrow S_0$, $\tilde{a}\,^3A'' \leftarrow \tilde{X}\,^1A'$, results from an $n \rightarrow \pi^*$ electron promotion and gives rise to a pattern of vibronic bands that can be attributed to activity of the methyl torsion and the aldehyde hydrogen out-of-plane wagging modes. Potential and kinetic energy surfaces were mapped out for the aldehyde wagging (α) and the torsional (Θ) internal coordinates by using 6–31G* Hartree–Fock calculations in which the structural parameters were fully relaxed. The potential and kinetic energy data points were fitted to double Fourier expansions in α and Θ and were incorporated into a two-dimensional Hamiltonian operator. The spectrum was simulated from the transition energies and the Franck–Condon factors and was compared to the observed jet cooled LIP spectra. It was concluded that while the RHF procedure gives a good description to the ground state dynamics, the triplet state surface generated by the UHF method is too bumpy and undulating.

INTRODUCTION

In general, the higher electronic states of molecules exhibit a greater structural flexibility than do the corresponding ground electronic states. This nonrigidity is a direct consequence of the excitation process which promotes an electron from a bonding or nonbonding orbital to a molecular orbital which is antibonding. Thus the $n \rightarrow \pi^*$ electronic excitation in the carbonyl chromophore results in a reduction of the C=O bond order from 2.0 to 1.5, while at the same time the bond length increases by 0.08–0.11 Å. Even more dramatic changes occur in the bond angle relationships. In the case of the molecular prototype,[1] formaldehyde CH_2O, the rigid planar conformation of the S_0 ground electronic state converts into a pyramidal structure on excitation. The out-of-plane motion that inverts the pyramidal S_1 singlet excited state structure is described by a double minimum potential which contains a central barrier of 350 cm^{-1}. The heights of the barriers to molecular inversion are sensitive to the nature of the attached group. For example, the first singlet and triplet states of the sulphur analog, thioformaldehyde CH_2S, are pseudoplanar, while formyl fluoride CF_2O, on the other hand, has a barrier of 3100 cm^{-1} to molecular inversion.

Additional large amplitude motion is introduced into these systems when more complex structures are attached to the carbonyl group. In the case of acetaldehyde, CH_3CHO, the CCHO frame is rigidly planar in the S_0 state and the rotation of the methyl group constitutes the single large amplitude mode. As would be expected, the molecular frame in S_1 acetaldehyde is pyramidal and the structure is highly flexible along both the aldehyde wagging and methyl torsion coordinates. Thus the low frequency dynamics of the excited state are governed by two large amplitude modes: torsion of the methyl group; and a wagging motion of the aldehyde hydrogen. An even more complex case would be acetone, $(CH_3)_2CO$, where the low frequency dynamics of the ground state are described by interacting methyl groups. Additional flexibility is introduced into the upper excited states from the wagging displacement of the carbonyl group. Thus it would require three large amplitude coordinates to describe the dynamics of excited states of this simple molecule.

It is the Franck–Condon principle that makes electronic spectroscopy an ideal tool for investigating large amplitude motions in polyatomic molecules. This principle relates the assignment of the observed band progressions to the normal coordinates that most closely correspond to the changes in molecular structure which occurs on electronic excitation. Thus we anticipate that the CH wagging and the CH_3-torsion modes would be active in forming progres-

[a]To whom correspondence should be addressed.
[b]Permanent address: Quantum Electronics Laboratory, Institute of Physics, A. Mickiewicz University, Grunwaldzka 6, 60-780 Poznan, Poland.

 0021-9606/92/183964-09$006.00 © 1992 American Institute of Physics

sions in the $S_0 \rightarrow S_1$ electronic spectrum of acetaldehyde.

The visible spectrum of thioacetaldehyde[2,3] lies in the 630–560 nm region and results from an $n \rightarrow \pi^*$ electron promotion. Both the spin allowed $S_0 \rightarrow S_1$ and spin forbidden $S_0 \rightarrow T_1$ transitions are observed in absorption and have about the same strength. As a result of the structural differences between the ground and excited electronic states, the vibronic fine structure contained in the absorption spectrum is found to be highly complex. In the case of the lower $S_0 \rightarrow T_1$ system,[4,5] the spin-orbit selection rules limit the number of active vibronic transitions, and thereby reduce the complexity of the spectra. At room temperature, this system consists of two clusters of bands that are separated by a quantum of the C=S stretching mode, Q_9'. The dense cluster that is located in the region of the system origin has been attributed to the activity of the methyl torsion mode, Q_{15}. Franck–Condon arguments suggest the appearance of this mode in the spectrum would result from a displacement of the equilibrium conformations in the two electronic states. The lower T_1 state is observed to be radiative and under collision free conditions has a lifetime[4] of about 10 μs.

EXPERIMENT

Thioacetaldehyde is unstable at room temperature. It may be prepared by pyrolysis of the trimer 1,3,5,-trimethyl-*s*-trithiane and detected in a flow system. In this case, the trimer was prepared by the method of Kroto *et al.*[7] by passing H_2S gas through an ice cold mixture of HCl and acetaldehyde. The CH_3CDO, CD_3CHO, and CD_3CDO samples were supplied by MSD isotopes. For CD_3CHS and CD_3CDS, which have exchangeable hydrogens DCl and D_2S, were used.

Jet-cooled phosphorescence excitation spectra of thioacetaldehyde and its deuterated isotopomers were obtained using the pyrolysis jet spectroscopic technique.[8] The crystalline trimer was warmed to 50 °C, the vapor entrained in 1 atm of argon, and the mixture pyrolyzed at 700 °C just prior to expansion through a 150 μ nozzle into vacuum. From past experience we estimate that rotational temperatures of 5–10 K were obtained under these conditions. In order to accentuate the weak hot bands, warm jet spectra also were recorded by altering the expansion conditions to prevent complete cooling of molecules in higher vibrational levels populated in the high temperature pyrolysis zone.

The phosphorescence of thioacetaldehyde was excited with a Nd:YAG pumped dye laser system (Lumonics HY 750+HyperDye 300) using rhodamine 6G, rhodamine 610, and coumarin 540A laser dyes (Exciton). Laser powers of 1–5 mJ per pulse and linewidths of approximately 0.1 cm^{-1} were employed. The emission was detected by imaging the cold portion of the supersonic expansion through a suitable cutoff filter to reject scattered light and onto a high gain, red sensitive photomultiplier (EMI 9816 QB). The excitation spectra were wavelength calibrated[9] by simultaneously observing the optogalvanic effect in a neon-filled hollow cathode lamp.

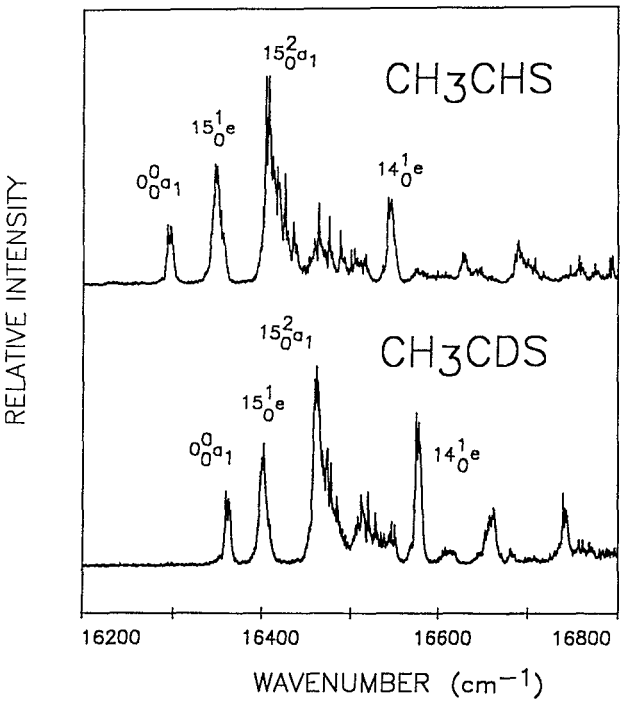

FIG. 1. The phosphorescence excitation spectra of CH_3CHS and CH_3CDS recorded under jet conditions.

RESULTS AND ASSIGNMENTS

Figures 1 and 2 show the phosphorescence excitation spectra of thioacetaldehyde and its deuterated isotopomers

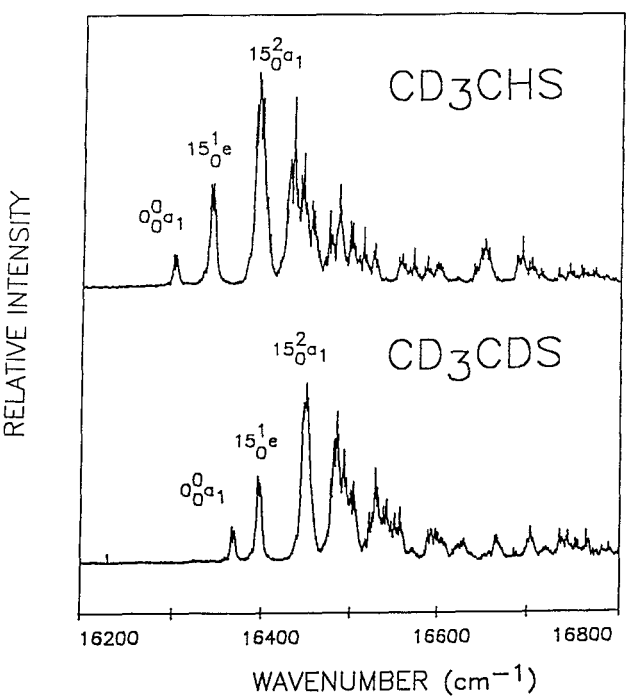

FIG. 2. The phosphorescence excitation spectra of CD_3CHS and CD_3CDS recorded under jet conditions.

TABLE I. Observed band maxima[a] in the excitation spectrum of (a) CH_3CHS, (b) CH_3CDS, (c) CD_3CHS, and (d) CD_3CDS.

Obs.	Diff.	Assign.[b]	Obs.	Diff.	Assign.	Obs.	Diff.	Assign.	Obs.	Diff.	Assign.
(a) Warm jet spectrum			(b) Warm jet spectrum			(c) Warm jet spectrum			(d) Warm jet spectrum		
159 87.2	−307.7	$15_2^0a_1$	158 47.1	−511.6		159 55.7	−344.0	15_3^0e	158 67.2	−500.0	14_1^0e
160 35.3	−259.6	15_2^1e	159 43.6	−415.1	15_3^0e	150 46.0	−253.7		158 87.1	−480.1	$14_1^015_0^2a_2$
161 31.9	−163.0	15_1^0e	160 57.6	−303.3	$15_2^0a_1$	160 58.4	−241.3	$15_2^0a_1$	160 30.4	−336.8	15_3^0e
161 88.7	−106.2	$15_1^1a_2$	160 72.4	−286.3		160 86.2	−213.5	15_2^1e	160 51.2	−316.2	$15_3^1a_2$
			162 00.8	−160.1	15_1^0e	162 13.4	−86.3	$15_1^1a_2$	161 07.4	−259.8	15_3^2e
Cold jet spectra			162 49.8	−111.1	$15_1^1a_2$	162 48.3	−51.4	15_1^2e	161 32.6	−234.6	$15_2^0a_1$
			162 92.6	−68.3	15_1^2e				161 57.4	−209.8	15_2^1e
						Cold jet spectra			162 11.2	−156.0	$15_2^2a_1$
162 94.9	0.0	$0_0^0a_1$							162 44.6	−122.6	15_1^0e
163 46.9	+52.0	15_0^1e	Cold jet spectra			162 99.7	0.0	$0_0^0a_1$	162 74.0	−93.2	$15_1^1a_2$
164 05.8	+110.9	$15_0^2a_1$				163 40.6	+40.9	15_0^1e	163 03.2	−65.0	15_1^2e
164 17.5	+122.6		163 60.9	0.0	$0_0^0a_1$	163 93.1	+93.4	$15_0^2a_1$			
164 26.1	+131.2		163 99.9	+39.0	15_0^1e	164 32.7	+133.0		Cold jet spectra		
164 35.5	+140.6		164 62.2	+101.3	$15_0^2a_1$	164 40.7	+141.0				
164 59.1	+164.2	15_0^2e	164 68.3	+107.4		164 43.8	+144.1		163 67.2	0.0	$0_0^0a_1$
164 63.6	+168.6		164 73.6	+112.7		164 53.7	+154.0	15_0^2e	163 96.8	+29.6	15_0^1e
164 75.5	+180.6		164 77.9	+117.0		164 73.2	+173.5		164 49.0	+81.8	$15_0^2a_1$
164 87.8	+192.9		164 84.6	+123.7	15_0^2e				164 81.6	+114.4	
164 99.6	+204.7		165 11.8	+150.9		164 84.5	+184.8		164 84.8	+117.6	
165 03.5	+208.3		165 19.8	+158.9		164 96.7	+197.0		164 92.5	+125.3	
165 16.3	+221.4		165 27.7	+166.8		166 50.1	+350.4		165 00.8	+133.6	15_0^2e
165 44.3	+249.4	14_0^1e	165 46.7	+185.8		166 91.9	+392.2		165 03.5	+136.3	
166 28.1	+333.2		165 27.7	+166.8		169 81.2	+681.5	$9_0^1a_1$	165 28.4,	+161.2	
166 89.7	+394.8	$10_0^115_0^2a_1$	165 46.7	+185.8		170 20.3	+720.6	$9_0^115_0^1e$	165 41.5	+174.3	
170 21.5	+726.6		165 76.7	+215.8	14_0^1e	170 72.0	+772.3	$9_0^115_0^2a_1$	165 51.2	+184.0	14_0^1e
170 42.1	+747.2	$9_0^1a_1$	166 62.1	+301.2	$14_0^115_0^1a_1$	171 11.7	+812.0		165 57.1	+189.9	
170 94.7	+799.8	$9_0^115_0^1e$	167 41.2	+380.3	$10_0^115_0^2a_1$	171 22.8	+823.1		167 03.3	+336.1	
171 53.8	+858.9	$9_0^115_0^2a_1$	170 82.2	+721.3	$9_0^1a_1$	171 31.8	+832.1		169 64.3	+597.1	
171 60.3	+865.4		171 23.6	+762.7	$9_0^115_0^1e$	171 33.9	+834.2		170 44.4	+677.2	$9_0^1a_1$
171 65.7	+870.8		171 53.7	+792.8	$8_0^1a_1$	171 51.3	+851.6		170 73.7	+706.5	$9_0^115_0^1e$
171 73.0	+878.1		171 86.6	+825.7	$9_0^115_0^2a_1$	171 62.4	+862.7	$9_0^115_0^2e$	171 25.3	+758.1	$8_0^1a_1$
171 82.9	+888.0	$9_0^115_0^2e$	171 96.9	+836.0		171 73.8	+874.1		171 56.3	+789.1	
172 10.8	+915.9		172 01.2	+840.2		172 03.5	+903.8		171 60.1	+792.9	
172 22.6	+927.7		172 08.0	+847.1	$9_0^115_0^2e$	172 43.3	+943.6		171 66.7	+799.5	$9_0^115_0^2a_1$
172 35.3	+940.4		172 34.8	+873.9					171 75.55	+808.3	
172 46.1	+951.2		172 42.5	+881.6					171 78.8	+811.6	
172 90.6	+995.7	$9_0^114_0^1e$	172 49.9	+889.0	$8_0^115_0^2a_1$				172 02.5	+835.3	$9_0^114_0^2e$
174 29.9	+1135.0		172 61.5	+900.6					172 26.6	+859.4	
175 13.1	+1218.2		172 66.1	+905.2					172 31.7	+864.5	
			172 72.3	+911.4							
			172 99.1	+938.2	$9_0^214_0^1e$						
			173 77.8	+1016.9							
			174 47.2	+1086.3							

[a]In cm^{-1}.
[b]See the text for notation.

recorded under jet-cooled conditions. Listings of the band maxima in the excitation spectra are given in Tables I(a) to I(d).

In contrast to the highly congested phosphorescence excitation spectra recorded earlier[4] at room temperature, the electronic origins ($0_0^0a_1$) of the singlet–triplet system can be identified without difficulty in the $CH_3CHS/CH_3CDS/CD_3CHS/CD_3CDS$ spectra as the onset of well defined bands at 16 294.9/16 360.9/16 299.7/16 367.2 cm^{-1}. The isotope effect on the origin band for CH_3/CD_3 methyl substitution is small ($+4.8/+6.3$ cm^{-1}), but somewhat larger for CHS/CDS substitution at the aldehyde end of the molecule, ($+66.0/+67.5$ cm^{-1}).

For shorter wavelengths, each isotopomer displays a simple progression in the cold jet spectrum which can be tracked out to two or three members. The first interval in the spectra of the four isotopomers is, respectively, $+52.0/+39.0/+40.9/+29.6$ cm^{-1}. On the basis of the low frequency interval and the CH_3/CD_3 isotope frequency shifts, these intervals can be assigned to the activity of the $\nu_{15}(C_s,a'')$ CH_3 torsional mode, 15_0^1e. The third band in the spectra of the isotopomers can be grouped into the progressions in intervals of $+110.9/+101.3/+93.4/+81.8$ cm^{-1} and bear the assignment $15_0^2a_1$. The corresponding intervals, 15_1^0e in the warm jet spectra which extend to longer wavelengths from the origin band are observed at $-163.0/-160.1/-122.6$ in the $CH_3CHS/CH_3CDS/CD_3CDS$ spectra.

As an aid to making the vibronic assignments, the molecular structures and vibrational frequencies of thioacetaldehyde were calculated by means of the GAMESS suite of *ab*

initio molecular orbital programs.[10] The restricted Hartree–Fock (RHF) and Unrestricted Hartree–Fock (UHF) schemes with a 6–31G* MO basis were employed for the S_0 and T_1 states. The structure for selected conformations of the two states were fully optimized. Vibrational frequencies were calculated in the harmonic approximation and scaled by 0.89 to correct for the effects of electron correlation.[11]

In the S_0/T_1 states, the C=S bond length was calculated to be 1.6064/1.7449 Å. The increase in C=S bond length of 0.1385 Å for $n\rightarrow\pi^*$ excitation is somewhat greater than would be expected for the 2.0 to 1.5 change in bond order of the thiocarbonyl group.[1] The structural change does suggest that the C=S mode should be strongly active in forming bands in the spectrum. The calculated T_1 state vibrational frequencies for the ν_9(C=S) vibration are 673.30/654.85/624.74/619.58 cm^{-1} for the four isotopomers. The intervals +747.2/+721.3/+681.5/+677.2 cm^{-1} that are observed between the prominent clusters which dominate the spectra are thus given the assignment $9_0^1a_1$.

The other interval which can be observed to form characteristic band clusters is found at +394.8 in the CH_3CHS spectrum. The CCS group is calculated to have an angle of 126.61° in the S_0 state, which decreases to 120.00° in the T_1 state. The ν_{10}(CCS) vibrational mode which most closely corresponds to this displacement is calculated to be 377.73 cm^{-1} in the S_0 state and 279.06 cm^{-1} in the T_1 state. Thus the cluster at +394.8 cm^{-1} is assigned to $10_0^1 15_0^2 a_1$. A set of bands is observed within the ν_9(C=S) group of torsional bands in CH_3CDS which is not found in CH_3CHS. The effect of D/H substitution allows the assignment to be made to the in plane ν_8(CCD) aldehyde hydrogen bend. The band at +889.0 cm^{-1} in CH_3CDS is assigned to $8_0^1 15_0^2 a_1$.

The final, and perhaps most interesting assignment, is that of the aldehyde out of plane wagging mode, ν_{14}. Assuming a rigid molecule of $C_s(a',a'')$ symmetry, the vibronic spin–orbit selection rules allow for only the $a'\leftrightarrow a'$ and $a''\leftrightarrow a''$ transitions. The moderately intense band at +249.4 cm^{-1} from the CH_3CHS origin, that shifts to +215.8 cm^{-1} in CH_3CDS, is assigned to the ν_{14} wagging mode. Based on the selection rules for the rigid C_s molecule, this single quantum of an a'' antisymmetric mode should not appear in the spectrum. However, the effect of the torsional nonrigidity splits the ν_{14} level into a_2 and e sublevels. As the vibrational zero point level of the S_0 state contains the a_1 and e sublevels an $e\leftrightarrow e$ transition can connect the lower electronic state with the single quantum addition ν_{14} of the T_1 state, $14_0^1 e$. What is surprising is that while this transition forms strong bands in the CH_3CHS and CH_3CDS spectra, the corresponding bands are weak or absent in the spectra of CD_3CHS and CD_3CDS.

To further understand the effects of the coupling of hydrogen wagging and methyl torsion, we simulated spectral profiles from the transition energies and Franck–Condon factors that were derived from *ab initio* Hartree–Fock calculations. The starting point for this analysis is the

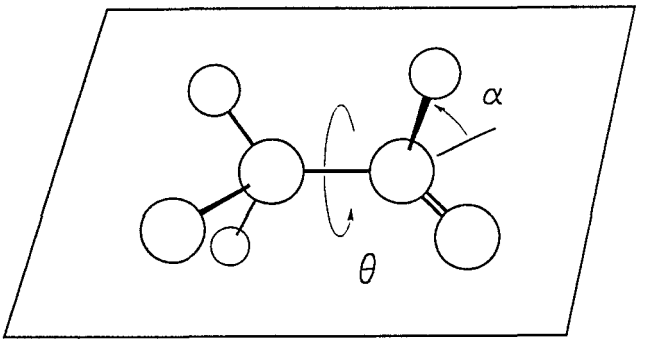

FIG. 3. The internal coordinates for the large amplitude motion: α (aldehyde wagging) and Θ (methyl torsion).

Hamiltonian operator, $H(\alpha,\Theta)$, for the combined wagging and torsional motions

$$\mathbf{H}(\alpha,\theta)=-\frac{\partial}{\partial\alpha}B_\alpha(\alpha,\theta)\frac{\partial}{\partial\alpha}-2\frac{\partial}{\partial\alpha}B_{\alpha,\theta}(\alpha,\theta)\frac{\partial}{\partial\theta}-\frac{\partial}{\partial\theta}B_\theta(\alpha,\theta)\frac{\partial}{\partial\theta}+V(\alpha,\theta). \quad (1)$$

In this equation $B_\alpha(\alpha,\Theta)$, $B_\Theta(\alpha,\Theta)$, and $B_{\alpha\Theta}(\alpha,\Theta)$ are the internal rotation constants and the kinetic interaction terms which depend on the α (hydrogen wagging) and Θ (methyl torsion) coordinates defined in Fig. 3. $V(\alpha,\Theta)$ is the potential energy.

The existence of symmetry planes in the methyl rotors and in the molecular frame allows the nonrigid symmetry of the S_0 and T_1 states of thioacetaldehyde to be classified[12] under the $\hat{C}_3$ torsion and $\hat{V}$ switch operations of the G_6 nonrigid group, where $\hat{C}_3 f(\alpha,\Theta) = f(\alpha,\Theta + 120°)$ and $\hat{V}f(\alpha,\Theta)=f(-\alpha,-\Theta)$. This is a group which is isomorphous with C_{3v}. It is therefore possible to block the matrix corresponding to Eq. (1) into a_1, a_2, and e representations.

The potential energy $V(\alpha,\Theta)$ may be described[2(a),2(b)] in terms of a Fourier series as

$$V(\alpha,\theta)=\sum_K\sum_L\left[A_{KL}^{CC}\cos K\alpha\cos 3L\theta+A_{KL}^{SS}\sin K\alpha\sin 3L\theta\right]. \quad (2)$$

A grid of energy data points[11] for the wagging and torsional coordinates was calculated using RHF and UHF methods for the S_0 and T_1 states. The molecular structure at each point was fully optimized. For the lower S_0 state, it was found that the series expansion could be limited to five terms,[11] whereas the excited state is relatively flat along the α and Θ directions and required a total of eight terms.

Plots of the potential surfaces are shown in Figs. 4 and 5. It is clear from these plots that the equilibrium conformation of lower S_0 state is planar with the aldehyde hydrogen and sulphur atoms eclipsed ($\alpha=0.0°,\Theta=0.0°$). The barrier to methyl rotation at the antieclipsed conformation ($\alpha=0.0°,\Theta=60.0°$) is calculated to be 541.44 cm^{-1}, which is to be compared to the observed microwave[1] value of 549.8 cm^{-1} and a value of 534.3 cm^{-1} obtained from the visible spectrum.[2] The steepness of the potential function in

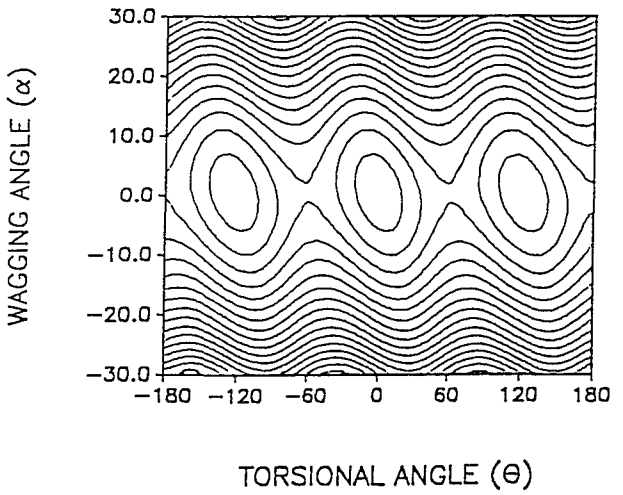

FIG. 4. The potential energy surface $V(\alpha,\Theta)$ for the S_0 electronic state. The interval between the contour lines is 200 cm^{-1}.

the direction of the α wagging coordinate indicates that Q_{14} is a small amplitude vibration in the lower electronic state.

The potential surface for the excited state is more complicated. In the equilibrium position, the C–H aldehyde bond is distorted from the CC=S plane by $+24.60°$, while at the same time the methyl group rotates by $+74.34°$. Thus a full cycle of the wagging–torsion coordinates generates six minima in the $V(\alpha,\Theta)$ potential surface for the T_1 state. The other interesting aspect of the energetics of the T_1 state is that the antieclipsed conformation is more stable than the eclipsed conformation by $321.79-175.55 = 146.24$ cm^{-1}. This change in the phase relationship in the potential functions for methyl rotation in the S_0 and T_1 states has been observed before[2(a)] and has been attributed to the effects of hyperconjugation.

While the kinetic energy contribution to the Hamiltonian is not as sensitive as the potential energy to changes

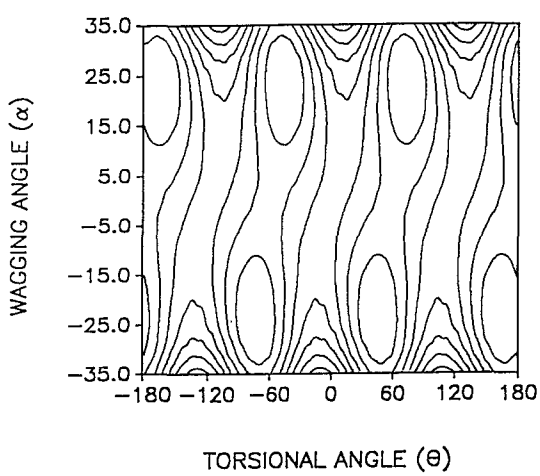

FIG. 5. The potential energy surface $V(\alpha,\Theta)$ for the T_1 electronic state. The interval between the contour lines is 100 cm^{-1}.

in the molecular structure, it does vary enough to be regarded as a constant. For this reason, the terms $B_\alpha(\alpha,\Theta)$ and $B_\alpha(\alpha,\Theta)$ as well as the interaction constant $B_{\alpha\Theta}(\alpha,\Theta)$ were evaluated at the same α,Θ grid points that were used to establish the potential surface. Since the molecular structure was fully optimized at each grid point, it is possible to evaluate the kinetic energy as a function of α and Θ by numerical methods.

To obtain the $B_\alpha(\alpha,\Theta)$ $B_\Theta(\alpha,\Theta)$, and $B_{\alpha,\Theta}(\alpha,\Theta)$ kinetic energy terms in Eq. (1), it is necessary to numerically determine the vibration–rotation **G** matrix. For the coupling of the two vibrations with the overall rotation, this is given by[13–15]

$$\mathbf{G}=\begin{bmatrix} I_{xx} & -I_{xy} & -I_{xz} & X_{11} & X_{12} \\ -I_{yx} & I_{yy} & -I_{yz} & X_{21} & X_{22} \\ -I_{zx} & -I_{zy} & I_{zz} & X_{31} & X_{32} \\ X_{11} & X_{12} & X_{13} & Y_{11} & Y_{12} \\ X_{12} & X_{22} & X_{32} & Y_{12} & Y_{22} \end{bmatrix}^{-1} . \tag{3}$$

The elements of this matrix are defined by

$$I_{ii}=\sum_{\alpha=1} m_\alpha(\mathbf{r}_\alpha\cdot\mathbf{r}_\alpha-r_{\alpha i}^2), \quad i=x,y,z, \tag{4}$$

where x, y, and z are the molecular fixed axes.

$$I_{ik}=\sum_{\alpha=1} m_\alpha r_{\alpha i} r_{\alpha k}, \quad i\neq k, \tag{5}$$

$$X_{ik}=\sum_{\alpha=1}^{N} m_\alpha\left[\mathbf{r}_\alpha\times\left(\frac{\partial\mathbf{r}_\alpha}{\partial q_k}\right)\right]_i, \tag{6}$$

and

$$Y_{ik}=\sum_{\alpha=1}^{N} m_\alpha\left(\frac{\partial\mathbf{r}_\alpha}{\partial q_i}\right)\cdot\left(\frac{\partial\mathbf{r}_\alpha}{\partial q_k}\right). \tag{7}$$

Here N is the number of atoms in the molecule, m_α is the mass of the αth atom, $\mathbf{r}_\alpha$ is the coordinate vector to the αth atom originating from the center of mass, and $r_{\alpha i}$ and $r_{\alpha k}$ are the ith and kth components of the αth vector, respectively. The derivatives defined in Eqs. (6) and (7) were numerically determined by calculating the structure of the molecule before and after increments of 0.01° were applied to the α and Θ directions as, $\alpha+\Delta\alpha$, $\alpha-\Delta\alpha$ and $\Theta+\Delta\Theta$, $\Theta-\Delta\Theta$. After the center of mass was determined, the elements of Eqs. (5)–(7) were inserted into Eq. (2), which was inverted to give the **G** matrix. The identification of the elements G_{44}, G_{55}, and G_{45} with the B_α, B_Θ, and $B_{\alpha,\Theta}$ internal rotation constants of Eq. (1) is the final stage of the calculation. The B_α, B_Θ, and $B_{\alpha,\Theta}$ constants were evaluated at the α and Θ grid points and were fitted to totally symmetric Fourier expansions.[11] Plots of the kinetic energy surfaces $B_\alpha(\alpha,\Theta)$ and $B_\Theta(\alpha,\Theta)$ for S_0 CH_3CHS are given in Fig. 6.

Figure 6 shows that the internal rotation constants for CH_3CHS in the two electronic states are nearly independent of the Θ and α coordinates. For example, $B_\Theta(\alpha = 0°,\Theta = 0°) = 7.570\,67$ for the eclipsed conformation decreases to $B_\Theta(\alpha = 0°,\Theta = 60°) = 7.551\,97$ cm^{-1} in the

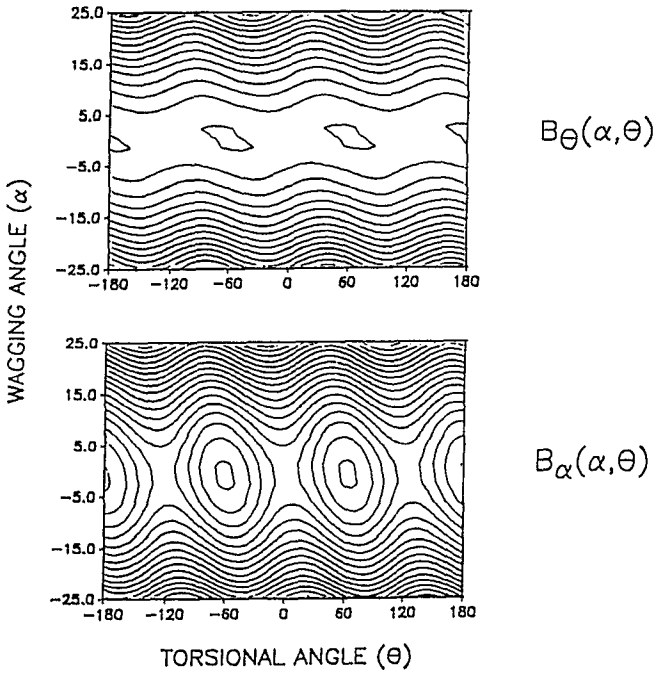

FIG. 6. Plots of the internal rotation constants $B_\alpha(\alpha,\Theta)$ and $B_\Theta(\alpha,\Theta)$. The contour intervals are 0.04 cm^{-1}.

antieclipsed form as the methyl group rotates by 60°. If the three methyl CH bonds are completely equivalent, the CH_3 group will have local C_3 symmetry and will behave as a finely balanced propeller as it rotates about the C–C bond. Under these circumstances the kinetic energy will be a constant of the motion and B_Θ will be independent of Θ. The calculated structures given in Ref. 9 for the eclipsed conformation show that the in-plane and out-of-plane CH bonds have different lengths, 1.0805 and 1.0874 Å, respectively, and change to 1.0831 and 1.0842 Å on rotation to the antieclipsed conformation. The 0.2% variation observed in the B_Θ values is a reflection of the unbalancing of the C–H propeller blades. The variation from $B_\alpha(\alpha = 0°,\Theta = 0°) = 17.2134$ to $B_\alpha(\alpha = 30°,\Theta = 0°) = 17.9732$ as the aldehyde hydrogen moves out of the plane is considerably greater than the changes which occur for methyl rotation. In this case, the CH group acts as a propeller with one blade which is not completely balanced. The result is that, as the CH group rotates, the center of mass of the molecule oscillates, which leads to large variations in the kinetic energy.

TABLE II. Calculated torsion–wagging energy levels for the S_0 and T_1 electronic states of thioacetaldhyde-h_4 with fixed and variable kinetic energy (in cm^{-1}).[a]

ν_{14}	ν_{15}	Sym.	S_0 (Fix.)[b]	S_0 (Var.)[c]	T_1 (Fix.)[d]	T_1 (Var.)[c]
0	0	a_1	0.000	0.000	0.000	0.000
0	0	e	0.018	0.203	0.215	0.213
0	1	e	151.806	152.012	82.398	82.645
0	1	a_2	152.504	152.720	84.328	84.654
0	2	a_1	283.172	283.369	173.092	172.706
0	2	e	290.526	290.922	166.186	167.238
0	3	e	389.101	389.297	190.531	190.243
0	3	a_2	429.315	430.230	171.290	172.500
1	0	a_2	860.861	864.064	313.846	313.361
1	0	e	860.926	864.148	254.337	253.861
1	1	e	994.121	997.205	300.930	302.371
1	1	a_1	995.704	998.976	347.882	347.994

[a]Expansion coefficients of $V(\alpha,\Theta)$ from Ref. (9).
[b]$B_\alpha = 17.1836$; $B_{\alpha,\Theta} = -2.469\,40$; $B_\Theta = 7.545\,45\ cm^{-1}$.
[c]Coefficients $B_\alpha(\alpha,\Theta)$, $B_{\alpha,\Theta}(\alpha,\Theta)$, and $B_\Theta(\alpha,\Theta)$ from Ref. (9).
[d]$B_\alpha = 16.6484$; $B_{\alpha,\Theta} = -1.796\,73$; $B_\Theta = 6.990\,67\ cm^{-1}$.

The wagging torsional Hamiltonian, Eq. (1), was solved by the variational method. It was found that 37 functions for torsion and 31 for wagging gave a sufficient basis size. Under the symmetrization of the G_6 group, the dimensions of the 1147×1147 direct product matrix were reduced to $a_1 = 202 \times 202$, $a_2 = 201 \times 201$, and $e = 2(372 \times 372)$.

DISCUSSION

In Table II, the energy level data obtained with flexible kinetic energy is compared to level data calculated with fixed kinetic energy. For the S_0 state, the first quantum of methyl torsion, $\nu_{15} = 1e$, was found to lie at 151.806 cm^{-1} for constant kinetic energy and to increase to 152.012 cm^{-1} for the variable kinetic energy case. It is possible to attribute this small difference in energy to the coordinates of the methyl torsion mode. The value for the internal rotation constant at the equilibrium conformation, $B_\Theta(0.0°,0.0°) = 7.570\,67\ cm^{-1}$ barely changes as the methyl group rotates by 60° to the staggered conformation, $B_\Theta(0.0°,59.97°) = 7.551\,97\ cm^{-1}$. As discussed previously, this result is a consequence of the mechanical balance of the CH methyl bonds as they rotate about the C–C axis. The internal rotation constant, however, is more sensitive to the effects of aldehyde wagging and increases to $8.246\,00\ cm^{-1}$ as α moves from the plane by 30°.

The potential surface of the T_1 excited state is broader and flatter than the S_0 ground state and contains six minima. The out-of-plane motion therefore extends over relatively large values of the α and Θ coordinates and the calculated frequencies would be expected to be more sensitive to variations in the kinetic energy. This, however, is not the case. Compare $\nu_{15} = 1e$ which is 82.398 cm^{-1} for fixed kinetic energy with the value of 82.645 cm^{-1} for the variable kinetic energy.

The energy level data of Table II can be used to assign the weaker bands. The experimental data for the lower S_0 state comes from the hot jet spectra of Table I(a). The observed values for the $\nu_{15} = 1e$ and $\nu_{15} = 2a_1$ levels, 163.0 and 307.7 cm^{-1}, compare favorably with the calculated values of 151.806 and 283.172 cm^{-1}, and indicate that the RHF procedure with a relaxed geometry provides a good description of the S_0 state.

For the T_1 state, however, the UHF procedure gives intervals of 82.398 and 173.092 cm^{-1} for $\nu_{15} = 1e$ and $\nu_{15} = 2a_1$, which are considerably higher than the observed values of 52.0 and 110.9 cm^{-1}. On the other hand, the $\nu_{14} = 1e$ quantum of wagging calculated at 254.337 cm^{-1} is well reproduced in the spectrum at 249.4 cm^{-1}. Thus it appears that the calculations generate a T_1 potential sur-

TABLE III. Calculated and observed torsion–wagging energy Levels for the S_0 and T_1 electronic states of thioacetaldhyde[a] (in cm^{-1}).

			CH_3CHS		CH_3CDS	
ν_{14}	ν_{15}	Sym.	S_0[b]	T_1[c]	S_0[b]	T_1[c]
0	0	a_1	0.00	0.00	0.00	0.00
0	0	e	0.00	0.75	0.00	0.62
0	1	e	170.66(163.0)	58.00(52.0)	167.01(160.1)	35.96(39.0)
0	1	a_2	170.99	62.90	167.21	37.87
0	2	a_1	321.45(307.7)	129.99(110.9)	317.01(303.3)	121.03(101.3)
0	2	e	325.75	148.81	319.76	127.08
0	3	e	444.06	184.89	441.83	144.89
0	3	a_2	473.10	201.04	462.65	147.17
1	0	a_2	863.64	288.80	626.19	252.21
1	0	e	863.66	237.83(249.4)	626.19	204.12(215.8)
B_α			17.183 6	16.648 4	8.634 03	8.453 28
$B_{\alpha,\Theta}$			−2.469 40	−1.796 73	−1.254 75	−0.985 16
B_Θ			7.545 45	6.990 67	6.862 59	6.302 03
			CD_3CHS		CD_3CDS	
ν_{14}	ν_{15}	Sym.	S_0[b]	T_1[c]	S_0[b]	T_1[c]
0	0	a_1	0.00	0.00	0.00	0.00
0	0	e	0.00	0.08	0.00	0.08
0	1	e	126.49	37.02(40.9)	121.85(122.6)	22.13(29.6)
0	1	a_2	126.50	37.62	121.85	22.37
0	2	a_1	245.12(241.3)	98.03(93.4)	236.78(234.6)	90.77(81.8)
0	2	e	245.19	102.91	236.82	93.63
0	3	e	353.99(344.0)	138.87	343.32(336.8)	114.45
0	3	a_2	354.94	155.12	343.76	119.51
1	0	a_2	820.01	213.66	603.89	180.62
1	0	e	820.03	196.13	603.89	162.58(184.0)
B_α			15.598 8	15.603 5	8.016 29	8.004 46
$B_{\alpha,\Theta}$			−1.133 04	−0.964 59	−0.751 48	−0.644 20
B_Θ			3.718 69	3.589 86	3.380 02	3.311 26

[a]Observed values are given in parentheses.
[b]S_0: $A_{00}^{CC}=20\,033.3$, $A_{10}^{CC}=-19\,713.6$, $A_{13}^{CC}=200.86$, $A_{23}^{CC}=-520.595$, $A_{13}^{SS}=700.397$.
[c]T_1: $A_{00}^{CC}=9210.82$, $A_{10}^{CC}=-10\,835.3$, $A_{13}^{CC}=495.771$, $A_{23}^{CC}=-474.227$, $A_{13}^{SS}=36.425$, $A_{30}^{CC}=1323.175$, $A_{33}^{CC}=5.992$, $A_{33}^{SS}=190.008$.

face which is adequately described in the α (aldehyde wagging) direction, but is too undulating and bumpy in the Θ (methyl torsion) direction.

The calculations provide a good starting point for a refinement of the potential functions. As the Fourier expansions contain too many terms for a complete least squares fitting of the data, it was necessary to choose a convenient set for adjustment. Expansion coefficients A_{13}^{CC}, A_{23}^{CC}, and A_{13}^{SS} were selected for scaling in both states. The A_{00}^{CC} constant was adjusted to set the equilibrium positions to zero energy. A global fit was made simultaneously to the observed energy level data of all four isotopomers. The results are shown in Table III.

The intensities of the transitions between the wagging–torsion levels of the S_0 and T_1 states were calculated from the Franck–Condon and the Boltzmann factors. The intensities calculated for a vibrational temperature of 30 K are given in Table IV. The spectra simulated with the 6–31G* and 6–31G* scaled models are compared to the experimental spectrum in Fig. 7. The bands of the excitation spectra have a distinct contour which is the result of the overlap of many rovibronic transitions. For the sake of comparison with the experimental spectrum, it was assumed that, under the low resolution used here, each band could be simulated by a Lorentzian function with a width at half-height of 10 cm^{-1}. While this procedure seems to be satisfactory for the lower bands in the spectrum, the contour of the 15_0^2e band appears to be quite different and extends over a 50 cm^{-1} range in a series of weak subbands. The upper level for this particular transition, $\upsilon_{15}=2e$, lies above the top of the barrier and as a result the methyl group undergoes nearly free rotation. Above the barrier the molecule acquires an additional degree of rotational freedom and an extra free rotation quantum number which has the effect of spreading the rotational fine structure over a wide range. As our model does not treat the case of free rotation, we have simulated the profile of these bands with a contour of 50 cm^{-1} width at half-height.

The agreement between the overall profiles of the observed spectrum and that calculated with the scaled 6–31G* basis (middle trace) is quite good, in that all of the major features are reproduced. The first band in the spectrum is composite and is calculated to consist of the two internal rotation doublets $0_0^0a_1$ and 0_0^0e with intensities of 8.2 and 4.3 which are separated by 0.75 cm^{-1}. The next

TABLE IV. Calculated transition energies[a] and intensities[b] for the methyl torsion and aldehyde wagging modes in the $S_0 \rightarrow T_1$ system of thioacetaldehyde, $T=30$ K.

CH_3CHS			CH_3CDS		
	cm^{-1}	Int.		cm^{-1}	Int.
15_0^2e	148.81	100.0	15_0^2e	127.08	100.0
$15_0^2a_1$	129.99	79.8	14_0^1e	204.12	70.0
15_0^1e	58.00	48.9	$15_0^2a_1$	121.02	58.7
14_0^1e	237.83	41.0	$15_0^4a_1$	204.12	31.0
15_0^3e	184.89	36.1	15_0^1e	35.95	21.2
$15_0^4a_1$	259.65	31.9	$14_0^1 15_0^1a_1$	277.84	10.8
$0_0^0a_1$	0.00	8.2	$0_0^0a_1$	0.00	6.3
0_0^0e	0.75	4.3	0_0^0e	0.62	3.3
CD_3CHS			CD_3CDS		
15_0^3e	138.87	100.0	15_0^4e	162.59	100.0
15_0^4e	196.13	49.9	15_0^3e	114.46	53.8
$15_0^4a_1$	178.81	44.1	$15_0^4a_1$	161.57	47.5
15_0^2e	102.91	25.4	15_0^2e	93.63	18.7
15_0^2e	98.03	24.2	$15_0^2a_1$	90.76	18.2
15_0^1e	37.02	11.3	Xa_1	220.72	11.3
Xa_1	332.06	4.3	Xa_1	284.30	9.3
Xa_1	281.61	3.7	15_0^1e	22.31	6.4
$0_0^0a_1$	0.00	1.1	$0_0^0a_1$	0.00	1.2
0_0^0e	0.08	0.9	0_0^0e	0.08	0.9

[a]Relative to $0_0^0a_1$.
[b]Strongest band scaled to 100.

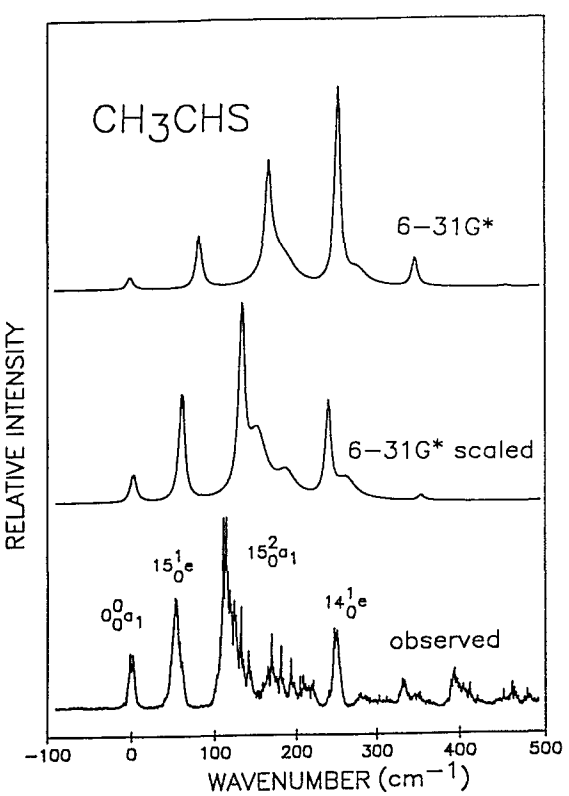

FIG. 7. A comparison of the observed and calculated supersonic jet spectra of CH_3CHS.

band, 15_0^1e, at $+52.0$ cm^{-1}, can be regarded as the first quantum addition of the ν_{15} torsional mode. Its torsional component, $15_1^1a_2$, does not appear in the spectrum since the low temperature of the jet allows for only the population of the two lowest levels: $v=0a_1$ and $v=0e$. The next band, $15_0^2a_1$, at $+110.9$ cm^{-1} forms the third member of the progression. The length and the strength of this progression in ν_{15} provides a measure of the displacement of the equilibrium structure which occurs on $S_0 \rightarrow T_1$ excitation. On the basis of Franck–Condon arguments, it may be concluded that the length and strength of the torsional progression calculated in the unscaled *ab initio* procedure is too great and that the changes in Θ are too large.

The potential energy surface of Fig. 5 shows that there are four routes by which the minimum energy configuration of the T_1 upper state can be achieved from the ($\alpha=0.0°, \Theta=0.0°$) configuration of the S_0 state, namely, the clockwise–clockwise ($+24.68°, +74.34°$), and counterclockwise–clockwise ($+24.68°, -45.66°$), rotations, and the equivalent set defined by the switch operator ($-24.68°, -74.34°$) ($-24.68°, +45.66°$). Thus it is possible for the structural displacement to occur along either the upward sloping positive diagonal or alternatively along the negative sloping diagonal. As the preference would be for a minimum structural distortion on electronic excitation, the structural changes would take place along the ($+24.68°, -45.66°$) ($-24.68°, +45.66°$) negative sloping diagonal. Fitting the simulated, (6–31G* scaled) to the observed spectra generates a potential which has a corresponding minimum at ($+22.38°, -41.08°$). In this case the minimum in the scaled potential is closer to the ground state origin by $\Delta\alpha = 24.68° - 22.38° = 2.30°$ and $\Delta\Theta = 45.66°$

TABLE V. Spectroscopic parameters for thioacetaldehyde (in cm^{-1}).[a]

	CH_3CHS			CH_3CDS	
	Obs.	Calc.		Obs.	Calc.
			S_0 State		
ν_{15}(tor.)	163.0	170.66		160.1	167.01
$2\nu_{15}$(tor.)	307.7	321.45		303.3	317.01
			T_1 State		
ν_{15}(tor.)	52.0	58.00		39.0	35.96
$2\nu_{15}$(tor.)	110.9	129.99		101.3	121.03
ν_{14}(wag.)	249.4	237.83		215.8	204.12
ν_9(C=S)	747.2	673.30		721.3	654.85
ν_{10}(CCS)	283.9	279.06		279.0	275.08
	CD_3CHS			CD_3CDS	
			S_0 State		
ν_{15}(tor.)				122.6	121.85
$2\nu_{15}$(tor.)	241.3	245.12		234.6	236.78
			T_1 State		
ν_{15}(tor.)	40.9	37.02		29.6	22.13
$2\nu_{15}$(tor.)	93.4	98.03		81.8	90.77
ν_9(C=S)	681.5	624.74		677.2	619.58
ν_8(CCH_a)		832.51		751.8	781.49

[a] T_1 state: 6–31G* scaled potential, maxima, and minima. $V(22.38°, -41.08°) = V(22.38°, +78.92°) = 0.00$; $V(0.0°, 0.0°) = 246.58$; $V(0.0°, 60.0°) = 192.50$; $V(22.38°, 18.92°) = 452.06$.

$-41.08° = 4.58°$. This smaller value of the Θ displacement then accounts for the reduced Franck–Condon activity which is observed in the torsional progression in the middle trace of Fig. 7. The other major difference is that the barrier to torsion along the $\alpha = 0.0°$ direction of 54.08 cm^{-1} is smaller than the 146.24 cm^{-1} value obtained for the *ab initio* case. This flatter potential is then directly responsible for the better agreement between the observed and calculated frequency intervals.

The observed and calculated spectroscopic parameters for the four isotopomers of thioacetaldehyde are collected together in Table V. We may conclude from the above results that the structure and dynamics which are derived from scaled 6–31G* *ab initio* theory provide a good starting point for both the assignment of the observed spectrum and the refinement of the simulated spectrum. While the RHF procedure gives a good description of the ground state structure and dynamics, the triplet potential surface generated by the UHF method is too bumpy and undulating. The UHF calculations also generate minima in the potential surface which are found to be greater than those observed at the T_1 position of equilibrium. Before a more detailed picture can be given of the intermode coupling in the excited T_1 state, it will be necessary to perform further studies at higher experimental resolution.

ACKNOWLEDGMENTS

D.C.M. and H. B. would like to thank the Natural Sciences and Engineering Research Council of Canada for financial support of this work. D.J.C. and J.K. acknowledge the support of the National Science Foundation through Grant No. CHE-8914403. Y. G. S. and A. N. wish to thank the Comision Interministerial de Ciencias y Technologia for economic support through Grant No. PB 90-0167.

[1] D. J. Clouthier and D. C. Moule, *Topics in Current Chemistry*, edited by K. Niedenzu (Springer, Berlin, 1989), Vol. 150, pp. 167–247.
[2] (a) R. H. Judge, D. C. Moule, A. E. Bruno, and R. P. Steer, J. Chem. Phys. **87**, 60 (1987); (b) Y. G. Smeyers, A. Nino, and M. N. Bellido, Theor. Chim. Acta **74**, 259 (1988); (c) Y. G. Smeyers, M. N. Bellido, and A. Nino, J. Mol. Struct. (Theochem.) **166**, 1 (1988); (d) H. W. Kroto and B. M. Landsberg, J. Mol. Spectrosc. **62**, 346 (1976).
[3] R. H. Judge, D. C. Moule, A. E. Bruno, and R. P. Steer, Chem. Phys. Lett. **102**, 385 (1983).
[4] A. E. Bruno, D. C. Moule, and R. P. Steer, J. Photochem. Photobiol. **46**, 169 (1989).
[5] D. C. Moule, Y. G. Smeyers, M. L. Senent, D. J. Clouthier, J. Karolczak, and R. H. Judge, J. Chem. Phys. **95**, 3137 (1991).
[6] Y. G. Smeyers, A. Nino, and D. C. Moule, J. Chem. Phys. **93**, 5786 (1990).
[7] H. W. Kroto, B. M. Landsberg, R. J. Suffolk, and A. Vodden, Chem. Phys. Lett. **29**, 265 (1974).
[8] J. R. Dunlop, J. Karolczak, and D. J. Clouthier, Chem. Phys. Lett. **151**, 362 (1988).
[9] M. L. Rutherford, D. J. Clouthier, and F. J. Holler, Appl. Spectrosc. **43**, 532 (1989).
[10] M. W. Schmit, J. A. Boatz, K. K. Baldridge, S. Koeseki, M. S. Gordon, S. T. Elbert, and B. Lam, QCPE Bull. **7**, 115 (1987).
[11] See AIP document no. PAPS JCPSA-97-3964-5 for 5 pages of tables Order by PAPS number and journal reference from American Institute of Physics, Physics Auxiliary Publication Service, 335 East 45th Street, New York, NY 10017. The price is $1.50 for each microfiche (98 pages) or $5.00 for photocopies of up to 30 pages, and $0.15 for each additional page over 30 pages. Airmail additional. Make checks payable to the American Institute of Physics.
[12] (a) Y. G. Smeyers, *Teoria de Grupos para Moleculas No Rigidas. El Grupo Local. Aplications.* Memorias, Vol. 13 (Real Academia de Ciencias, Madrid, 1989); (b) Y. G. Smeyers, *Introduction to Group Theory for Non-Rigid Molecules*, Advances in Quantum Chemistry, edited by P. O. Lowdin (Academic, New York, in press).
[13] T. B. Malloy, Jr. and L. A. Carreira, J. Chem. Phys. **71**, 2488 (1979).
[14] M. A. Harthcock and J. Laane, J. Chem. Phys. **79**, 2103 (1983).
[15] M. A. Harthcock and J. Laane, J. Phys. Chem. **89**, 4231 (1985).